J. Mountain Res. P-ISSN: 0974-3030, E-ISSN: 2582-5011 DOI: https://doi.org/10.51220/jmr.v20-i1.52
Vol. 20(1), (2025), 485-500

Hydrogeochemical and Geostatistical Evaluation of Groundwater Quality In Semi-Arid Region of Eastern Rajasthan: A PCA and Geospatial-Based Approach

Sunita[1] • Har Lal Singh[1] • Sunil Singh[1*] • Jitendra Binwal[1]

[1]*School of Liberal Arts and Sciences, Mody University of Science and Technology, Lakshmangarh-332311, Sikar, Rajasthan, India*

[*]**Corresponding Author Email Id:** sunilgeo.hnbgu@gmail.com

Received: 25.04.2025; Revised: 27.06.2025; Accepted: 30.06.2025

Abstract: The increasing demand for freshwater resources due to population growth and associated activities has exacerbated groundwater quality challenges, especially in semi-arid regions. This study evaluates the hydro-geochemical properties of groundwater in eastern Rajasthan, using geostatistical methods integrated with Principal Component Analysis (PCA) and geospatial techniques. A comprehensive field examination collected groundwater samples from 36 sites and assessed 14 hydro-geochemical parameters, including Sodium, Potassium, Calcium, Magnesium, pH, Total Hardness, TDS, Conductivity, Alkalinity, Nitrite, Bicarbonate, Fluoride, Chloride, Iron (Fe), and Depth. The majority of samples revealed Na-Cl-type characteristics with evaporation dominance. A strong positive association was observed between Na^+ and EC (r = +0.95) and between Alkalinity and HCO3- (r = + 0.94), while a negative association was identified between HCO3- and depth (r = -0.45) and between Ca++-Mg++ and pH (-0.43). In addition, Wilcox diagrams classified most groundwater sources as permitted to dubious. The PCA analysis identified four main components, accounting for 85.86% of the variance. Component 1 (40.41%) comprised Na^+, EC, TDS, HCO_3^-, and Alkalinity, whereas Component 2 (20.66%) contained TH, F^-, Ca^+-Mg^{++}, and K^+. These findings suggest that geochemical processes affect groundwater quality and that semi-arid regions require sustainable groundwater management.

Keywords: Ground-water quality • Semi-arid • PCA • Geospatial technology

Introduction

Groundwater has become the primary global water source due to population growth and diverse water demands (Adimalla & Li, 2019; Tizro & Voudouris, 2008; Qiu et al., 2023). Rapid urbanization has transformed landuse and increased water consumption across agriculture, housing and industry sectors (Kheirandish et al. 2020; Zhou et al., 2022; Singh et al., 2022), making water supply predominantly dependent on groundwater resources (Nihalani et al., 2022; Patra et al., 2018). Both natural and anthropogenic factors influence groundwater quality (Panahi et al. 2021; Wu et al. 2023; Zhu et al., 2012; Singhal et al., 2020), with scientists investigating seasonal variations in groundwater chemistry and pollution indices (Rao et al., 2022; Tiwari et al., 2024). Water quality deterioration increases costs for obtaining clean water and may cause water shortages.

The mobilization of groundwater solvents, such as fluoride and arsenic, together with deep groundwater origins and evolution, were investigated in the Yuncheng Basin, central China, using hydro-geochemical parameters and isotopes (Dong et al., 2022; Qiu et al., 2023; Gosh & Sunita, 2024). The Na-HCO_3-(SO_4) groundwater type, showing diverse compositions, originated from closed reducing environments and semi-closed facultative conditions, influenced by subsurface leaking and palaeo-recharge processes. The El Arich aquifer's hydro-geochemical properties were evaluated against WHO and Tunisian standards using multivariate methods (Du et al., 2014; Li et al., 2022; Wu et al., 2022). Only 17.65% of groundwater samples met consumption standards for TDS, Na+, K+, EC and F- parameters. Principal component analysis (PCA), widely used across scientific disciplines, reduces data dimensionality while retaining substantial information (Zhou et al. 2023; Ghosh et al., 2014; Xu et al., 2022; Ghosh and Sunita, 2024). The impact of human activities on groundwater at EI Arich was assessed using hydrochemical and geostatistical methods within a GIS framework, showing most samples were unsuitable for consumption due to high carbonate mineral concentrations (Liu et al., 2023; Nsiri et al. 2021; Ghosh and Sunita, 2024). Hydro-chemical characteristics of groundwater in Xinzhou Basin, Shanxi, North China, were analyzed using Piper diagrams, PCA, correlation analysis, chloro-alkaline indices, Gibbs diagrams, and ion proportion diagrams (Shuai et al., 2021, Yin et al., 2023, Zhou et al., 2022, Ghosh and Sunita, 2024). Results indicated sodium originated from Na-Ca exchange. Sodium adsorption ratio, soluble sodium percentage, and water quality index models assessed groundwater suitability for irrigation and consumption. Predominant hydrochemical facies were Mixed HCO_3-CaMgNa and HCO_3-Ca, with some areas showing HCO_3-SO_4-Cl-Na. Southern basin shallow groundwater may be suitable for agricultural and potable use. Hydrogeological investigations revealed fluoride and arsenic increase mechanisms in arid/semi-arid Tumochuan plain regions (Dong et al., 2022; Yin et al., 2023).

Multiple studies utilize statistical techniques like PCA, WQI, and t-tests to investigate water pollution determinants. Elemile et al. (2021) applied these methods, while WPI and WQI assessments in Andhra Pradesh, India showed substantial groundwater segments required urgent intervention for drinking suitability (Ravindra et al., 2023). Gugulothu et al., 2022 assessed nitrate and fluoride risks in rural Telangana, India, recommending fertilizer restrictions and rainwater collection. PCA identified three latent components in Nigerian groundwater for wet and dry seasons, clarifying seasonal variations in soil erosion and natural pollution while identifying organic matter oxidation and mineral dissolution as additional factors. Similar methodology was employed in Nagpur, India (Marghade et al., 2015), analyzing 36 samples pre- and during monsoon. TDS and TH values varied from extremely soft to very hard and fresh to saline. Unfit samples comprised 33% pre-monsoon and 36% post-monsoon. PCA categorized chemical variables into two groups, accounting for 62.09% and 61.33% of overall variation respectively. Ghosh and Kanchan (2014) assessed West Bengal groundwater using PCA and Hierarchical Cluster Analysis, finding greatest factor loadings in the eastern unconfined aquifer section. Rao et al. (2019) identified significant groundwater quality factors through PCA in Visakhapatnam suburbs, Andhra Pradesh. Rao and Chaudhary (2019) noted hydro-chemical process management as critical for groundwater contamination dispersion. Literature review reveals limited multivariate analysis in Rajasthan's semi-arid and arid regions, particularly the transitional plain of inland drainage. This study employed PCA and geospatial technology to categorize groundwater quality based on hydro-geochemical characteristics.

Methods and Materials

Study Area: The study area lies between 27°21'N to 28°31'N latitude and 74°44'E to 76° 06'E longitude with an area encompasses 13,660 km² (Figure 1). It borders Haryana, Churu, Nagaur and Jaipur from the north-east, north-west, south-west and south. The region has hot summers and cold winters with

 DOI: https://doi.org/10.51220/jmr.v20-i1.52

minimal precipitation. Arid climates dominate the norther part, while semi-arid climates dominate the south (CGWB 2017). The climate is hot and dry year-round with little precipitation and the soil is predominantly sandy or sandy loam; however, its texture varies across the region.

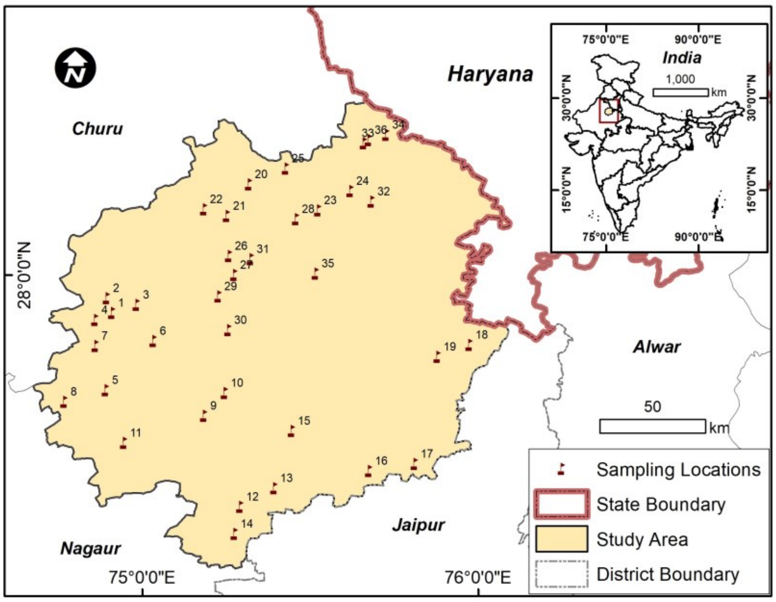

Figure 1. Location map of the study area.

Groundwater Sample Collection for Geochemical Analysis

In 2022, 36 groundwater samples were collected during pre-monsoon period using pre-cleaned 1-liter polyethylene containers from hand pumps, wells and tube wells. The sampling location was selected using a random sampling technique for consistent spatial coverage. Hand pumps and tube wells were purged for five to ten minutes to remove any residual standing water. Each sample container was marked with water-resistant ink, and relevant data was recorded for each sample. Then, Garmin GPS and Google Earth Pro were used to determine the sampling coordinates and unique identifiers of the locations. The samples were swiftly transported to the lab under low-temperature and solar-protected conditions. We used a water testing kit from the PHED laboratory in Sikar, Rajasthan, to measure pH, electrical conductivity (EC), fluoride (F^{-}), iron (Fe), nitrite ($NO2^{-}$), total hardness (TH) and total dissolved solids (TDS). E Additional parameters (Na^{+}, $Ca2^{+}$, $Mg2^{+}$, $HCO3^{-}$, Cl^{-}) were analyzed at the State Level Water Testing Laboratory in Jaipur using IARI Methods Manual 2005 protocols.

Statistical analysis and Methods

Descriptive statistical analysis, box-plots, and Pearson correlation analysis were conducted using R-studio, while hydrochemical results were visualized through Piper and Wilcox diagrams in Diagrammes software. Correlation matrices and heat maps were generated using R-studio's corrplot package and Gibb's diagrams were created in Microsoft Excel. Principal Component Analysis (PCA) was employed to reduce data dimensionality while preserving interrelated factors. Variables were categorized using the Kaiser Criterion (eigenvalues >1) and Scree test with Varimax rotation applied to maximize variability. The complete procedure was executed using Origin Pro software. The ArcGIS generated geographic representations of sampling locations with corresponding results. Inverse Distance Weighting provided spatial interpolation with appropriate classifications and PCA scores were similarly mapped within the ArcGIS environment.

J. Mountain Res. P-ISSN: 0974-3030, E-ISSN: 2582-5011 DOI: https://doi.org/10.51220/jmr.v20-i1.52
Vol. 20(1), (2025), 485-500

Principal component analysis (PCA)

PCA is a statistical technique that reduces dataset complexity while maintaining data integrity by converting original variables into uncorrelated, orthogonal components preserving maximum variance (Kumar et al., 2022). The PC1 represents maximum variation, with subsequent components showing diminished variances. The PCA was analysed using standard methodology (Jolliffi, 2002)

Results and Discussion

Aquifer Zones in the Study Area: The study area contains two primary aquifer systems: an unconfined aquifer dominating the northern region with a minor southern section, and a semi-confined aquifer in the south-central area (Figure 2). Older alluvium forms the main aquifer across the western section, while younger alluvium comprises a minimal portion. The northern aquifer consists primarily of quartzite and alluvium materials.

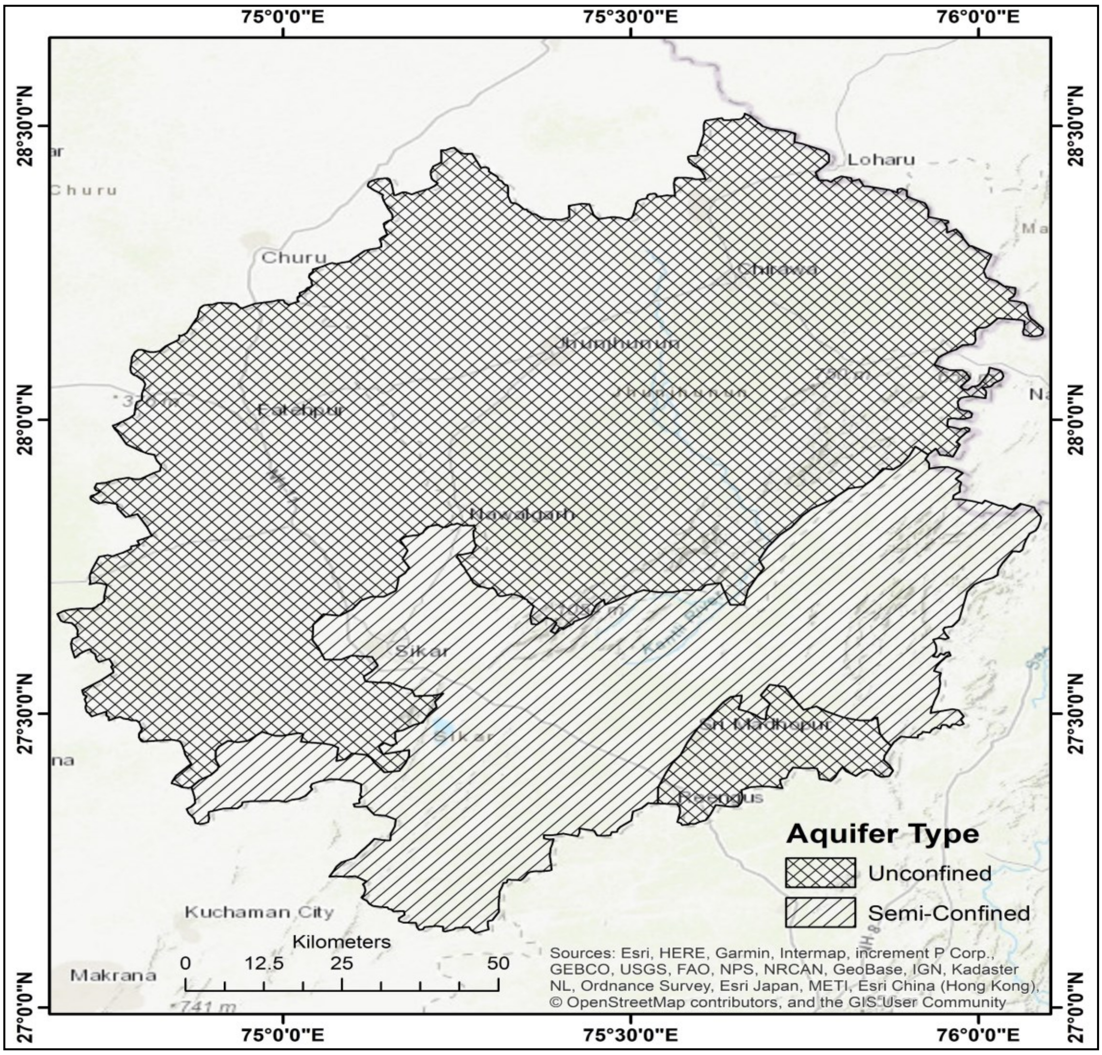

Figure 2. Aquifer zones in the study area.

Spatial Distribution and Overall Geochemical Characteristics

Descriptive statistics for specified parameters are shown in Figure 3 and Table 1. The pH level ranged from 7.2 to 8.7 with a mean of 7.8 and standard deviation of 0.30, indicating slightly acidic conditions. Table 2 presents drinking water quality parameters with corresponding BIS standards (Bureau of Indian Standards, 1991).

Table 1. Illustrating the descriptive statistics values of the parameters.

Parameters	pH	EC (ds/m)	TDS (mg/l)	TH(mg/l)	Fe (mg/l)	F- (mg/l)	Cl-(mg/l)	HCO3- (mg/l)	NO2-(mg/l)	Ca+Mg (mg/l)	K+(mg/l)	Na+ (mg/l)	Alkalinity (mg/l)	Depth (mbgl)
Mean	7.82	2.21	965.33	215.14	0.24	1.83	458.09	595.53	0.31	173.88	3.19	405.72	309.03	55.84
Min	7.2	0.55	366	80	0	0.5	56.72	170.83	0	45.5	0.32	48.26	120	4.7
Max	8.7	8.88	2658	1135	1	5	1729.96	1964.52	0.5	734.5	23.94	2019.94	870	98
SD	0.3	1.53	529.28	223.53	0.23	0.87	385.03	402.92	0.16	121.53	4.71	323.19	183.11	22.28
Skewness	0.34	2.82	1.61	2.89	1.38	1.37	2.24	1.61	0.28	3.08	3.33	3.71	1.71	-0.26

Table 2. Drinking water quality standards by BIS (Bureau of Indian Standards)

Parameters / BIS Limit	pH	EC	TDS	TH	Fe	F-	Cl-	HCO3-	NO2-	Ca2+	Mg2+	K+	Na+	Alkalinity
Desirable	6.5-8.5	-	300	300		1	250	-	-	75	30	-	-	-
Maximum Permissible	6.5-8.5	-	1500	600		1.5	1000	-	-	200	100	-	-	-

The unit of all the parameters are in mg/l except pH.

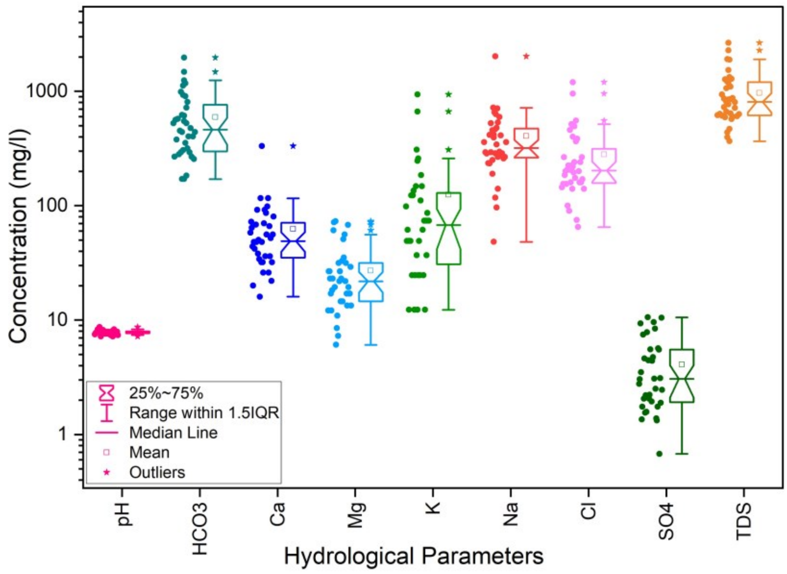

Figure 3. Descriptive statistics of groundwater parameters.

The pH exhibited moderate positive skewness (0.34), with higher concentrations in the northern region and natural quantities dominating most areas (Figure 4a). EC distribution was greater in the northern than western zone, ranging from 0.55-8.88 ds/m (mean: 2.21 ds/m, SD: 1.53 and skewness: 2.82), with elevated concentrations in southern and western regions (Figure 4b). The TDS levels were significantly higher throughout the study area except the middle section, ranging from 366-2658 ppm (mean: 965.33 ppm, SD: 529.28 and skewness: 1.61), showing a distinct spatial pattern from EC (Figure 4c). The TH concentrations ranged from 80-1135 ppm (mean: 215.14 ppm, SD: 223.53 and skewness: 2.89), peaking in central and eastern areas (Figure 4d). The iron concentrations averaged 0.24 ppm (SD: 0.23), with highest concentration found in northern and western parts and a minor area in the southeast (Figure 4e). The concentration of fluoride (F^-) ranged from 0.5-5 ppm, with an average of 1.83 ppm and a standard deviation of 0.87, indicating notable variation in concentration across the area. The skewness of fluoride exhibited a significantly positive value of 1.37, with a peak concentration of 5.00 ppm and a notably elevated mean of 1.83 ppm. The highest concentration of F- was noted in the peripheral regions, predominantly in the southern and western areas, as well as the northern section, whereas the central area exhibited a comparatively lower concentration (Fig 4f).

Chloride concentrations were highest in the southern region (56.72-1729.96 ppm, mean 458.09 ppm and SD 385.03) with positive skewness of 2.28 (Figure 4g). The HCO3- levels peaked in the western section (170.83-1964.52 ppm and 120.00-870.00 ppm, means 595.53 and 309.03 ppm respectively) showing positive skewness of 1.61 and 1.71 (Figure 4h). The concentration of Nitrite ranged from below the detection limit (BDL) to 0.50 ppm (mean 0.31 ppm, SD 0.16 and skewness 0.28) with higher concentrations in northern and western patches (Figure 4i). The Ca and Mg concentrations were elevated in northern and southern regions (45.50-734.50 ppm, SD 121.53 and 173.88 ppm respectively and skewness 3.08), while Na was predominantly high in the southern segment (mean 405.72 ppm) (Figure 4j). K^+ was highest in the eastern segment (0.32-23.94 ppm) (Figure 4k), whereas Na^+ was lower centrally but higher in southern and western areas (48.26-2019.94 ppm, mean 405.72 ppm) (Figure 4l). The Alkalinity was lower in the middle region but higher in southern and western areas (Figure 4m). Groundwater depth was greater in southern and northern regions compared to the central region (Figure 4n). Multiple correlation matrices showed moderate to strong positive relationships among selected parameters.

A robust positive correlation was found between F and EC (r = +0.72), Na and EC (r = +0.95), chloride and EC (0.94), chloride and TDS (0.87) and chloride and Na (0.86). Moderate positive correlations existed between HCO_3- and F^- (0.63), $HCO3^-$ and TDS (0.65), and alkalinity and EC. Negative relationships were predominantly moderate, including TDS and pH (r = -0.41), Ca + Mg and pH (r = -0.43), and NO_2 and EC (r = -0.34) (Figure 5). The Piper diagram analyzes hydro-geochemistry categories through anions and cations, comprising two triangles representing cation and anion facies and a rhombus encompassing the entire facies. The lower-left ternary figure (cation diagram) shows Ca_2+ predominance with Na^+ and K^+.

The Piper plot showed dominant sodium-type hydro-geochemical facies in groundwater samples. The anion diagram (lower-right ternary plot) revealed mixed chemistry including no dominant type, bicarbonate type, and chloride type. The comprehensive analysis of anions and cations reveals that the water exhibits characteristics of both NaCl type and Mixed Ca Na type (Figure 6). The Wilcox diagram illustrated that most samples fell within the good to excellent category, while a small number were classified as permissible to doubtful (Figure 7a & 7b). Only one sample was identified as unsuitable for drinking purposes. Gibbs (1970) provides valuable insights into the relationship between the lithological characteristics of an aquifer and the chemical composition of water. Gibbs diagrams are commonly employed in groundwater studies to clarify and understand the processes that affect water chemistry. The mechanisms involved relate to the hydrogeochemical composition shaped by precipitation, interactions between water and rock, and crystallization processes that occur during evaporation.

DOI: https://doi.org/10.51220/jmr.v20-i1.52

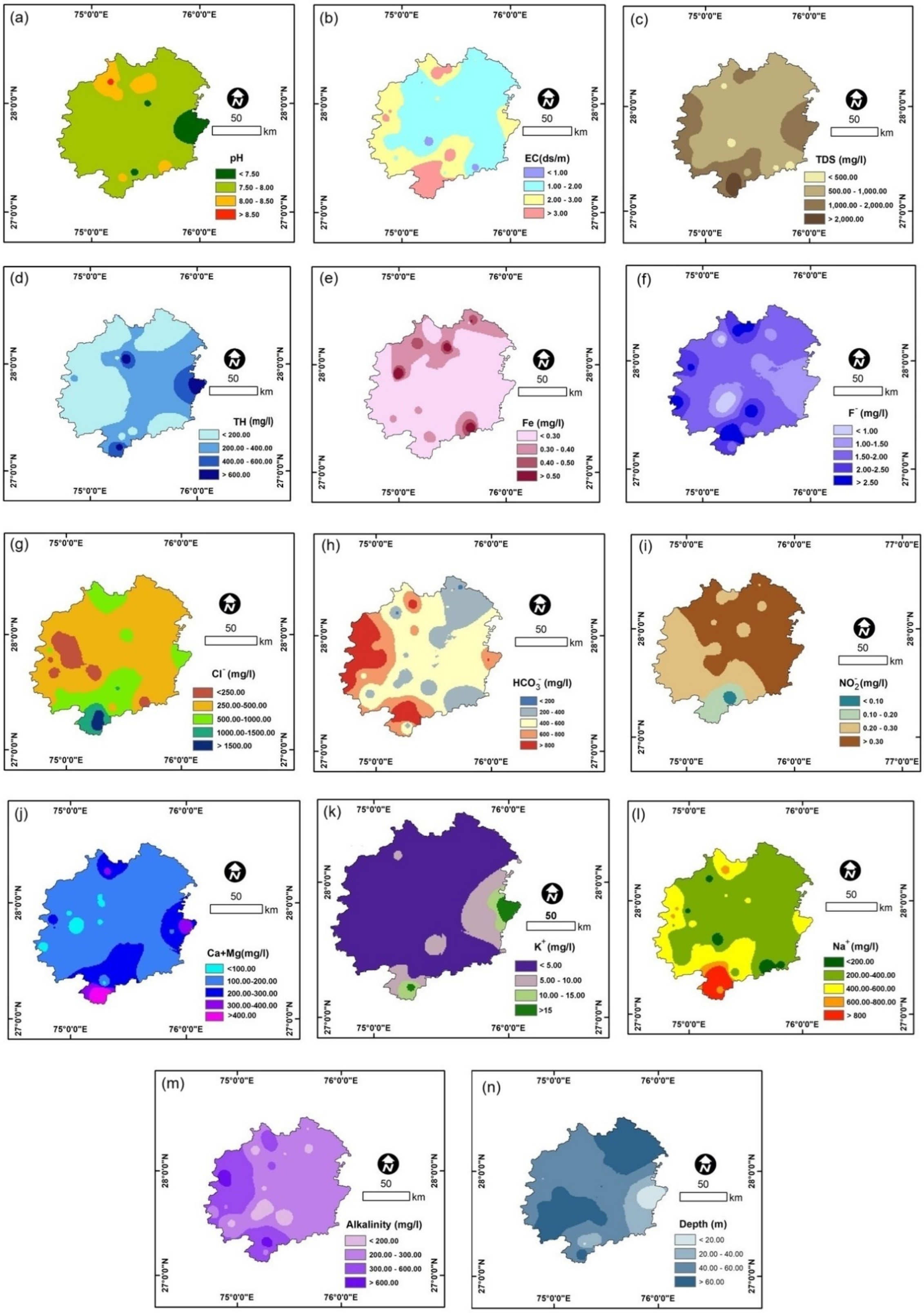

Figure. 4. Spatial distribution of physicochemical parameters [a] pH, [b] EC, [c] TDS, [d] TH, [e] Fe, [f] F^-, [g] Cl, [h] HCO_3^-, [i] NO^-_2, [j] Ca^+Mg, [k] K^+, [l] Na^+, [m] Alkalinity and [n] Depth.

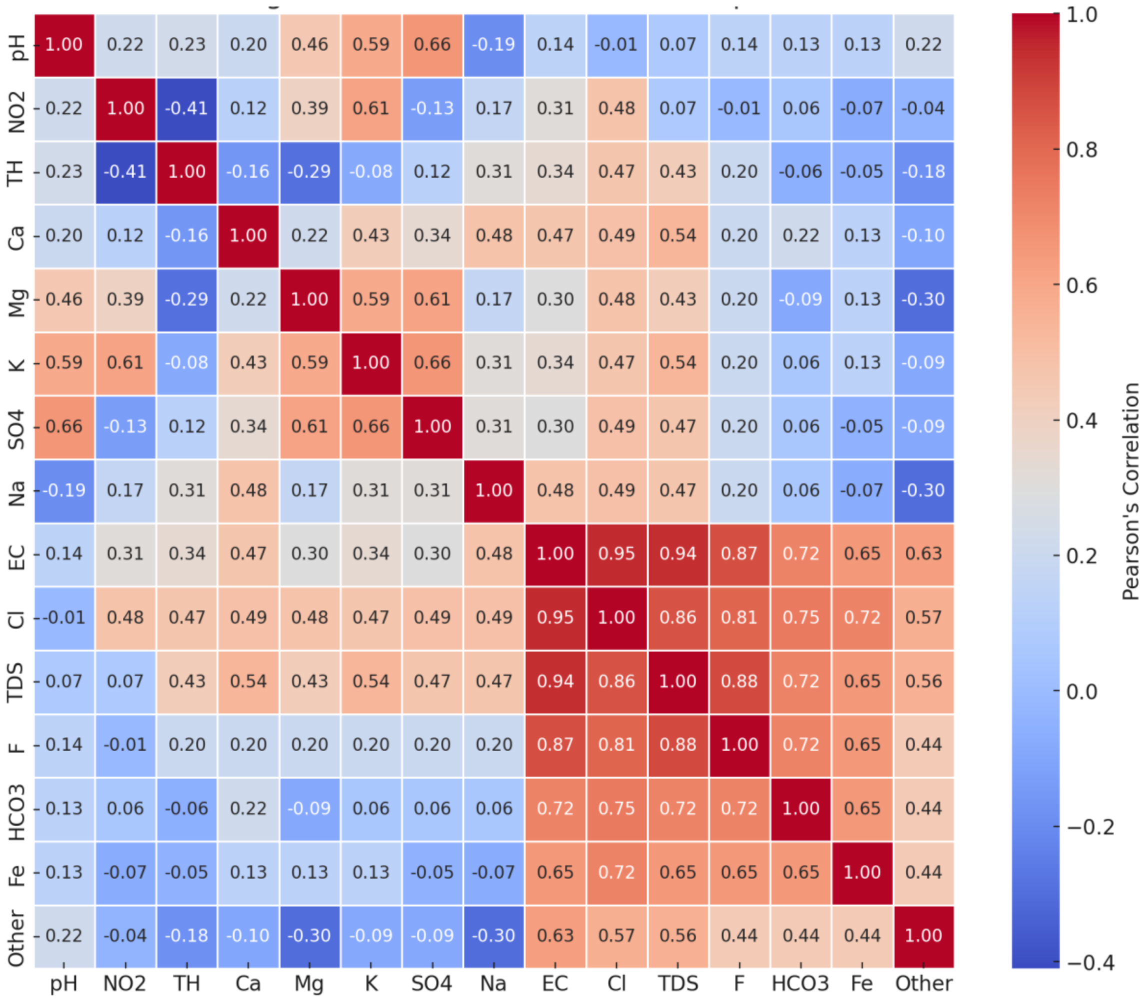

Figure. 5. Correlation matrix and heat map of specified hydro-geochemical parameters.

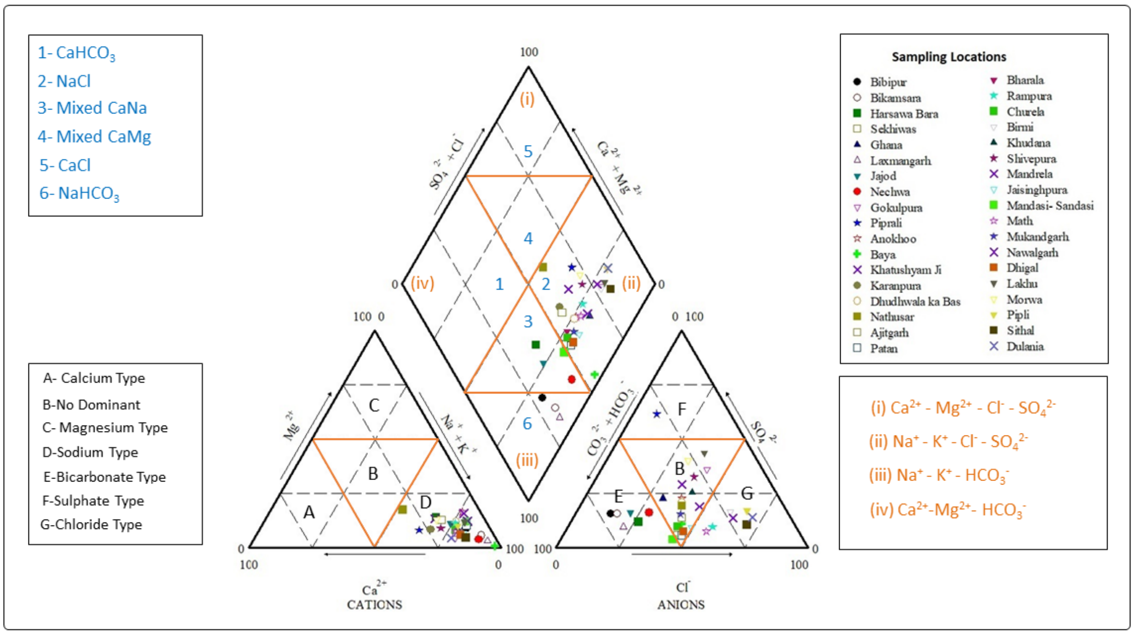

Figure 6. The Piper diagram showcases the hydro-chemical facies of groundwater.

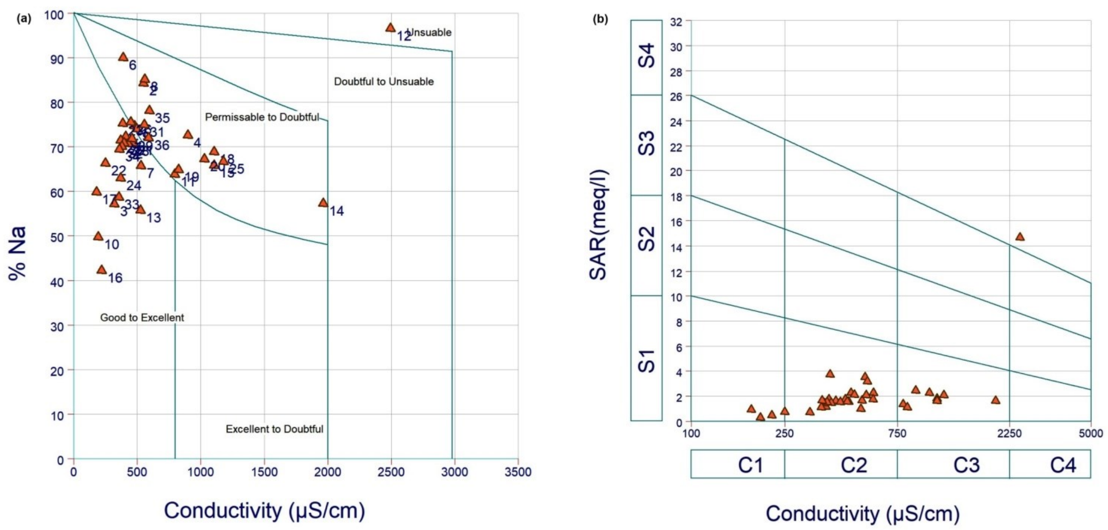

Figure. 7. Wilcox diagram depicting water quality.

The correlation between TDS and Na+/ (Na++Ca2+) demonstrates that the samples are positioned in the upper part of the graph, suggesting that evaporation primarily influences groundwater chemistry (Figure 8a and 8b). The correlation of samples in regions influenced by evaporation and rock significantly impacts groundwater chemistry, as demonstrated by the relationship between TDS and Cl/ (Cl- + HCO3-). The evaporation dominance zone in the current study area was where the majority of groundwater samples were collected, whereas only a limited number of samples were identified in the rock domination region. Given the dry and semi-arid conditions present in the study area, the findings indicate that evaporation is the main process occurring. The quality control was illustrated through the incorporation of a QC chart (Figure 9). The Lower Control Limit (LCL) and Upper Control Limit (UCL) were determined to be -3.321 and 486.1, respectively, in the analysis of the subgroup mean. Conversely, regarding the range, the lower control limit and upper control limit were observed at 301.2 and 1660, respectively. All of the samples exhibited values within the lower control limit and upper control limit, with the exception of two samples (sample no. 12 & 14). The findings indicated that the majority of the samples did not surpass the LCL and UCL thresholds.

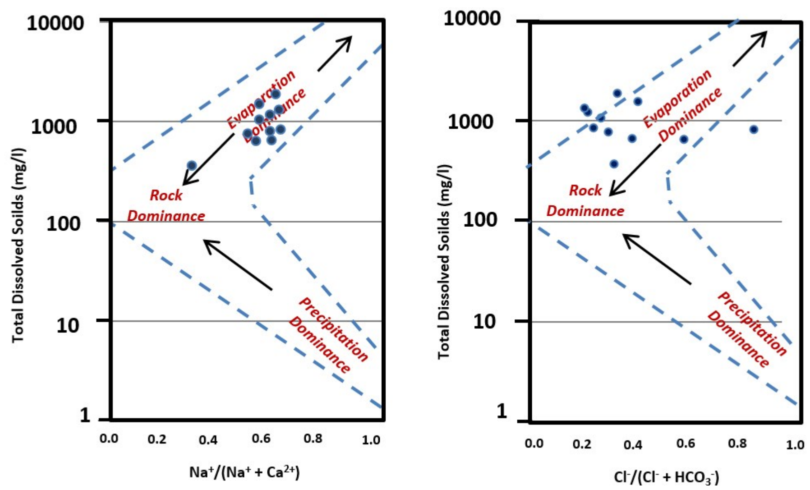

Figure 8. Gibb's diagram depicting groundwater chemical composition and lithological feature of aquifer.

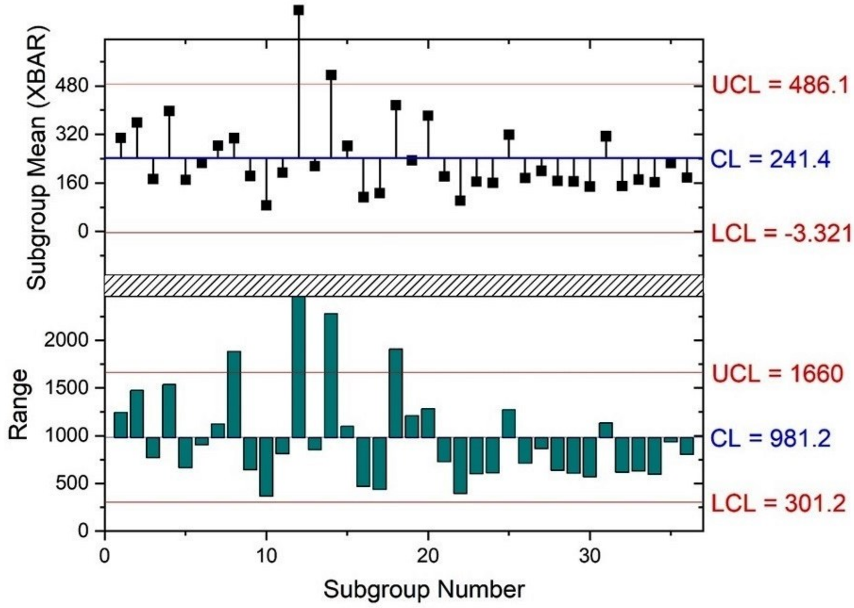

Figure 9. The QC chart showing the quality control of the data set

Principal Component Analysis (PCA) Results

Four main components were identified through varimax rotation, with eigenvalues exceeding one, accounting for 85.86% of the total variability in the data. Principal Component 1 exhibited a variance of 40.41%, showing higher positive loadings on the parameters EC (+0.404), TDS (+0.395), HCO3 (+0.313), Na (+0.385) and Alkalinity (+0.294). Principal Component 2 indicated that TH (+0.400), F^- (+0.292), $Ca^{++}Mg^+$ (+0.436), and K^+ (+0.478) parameters contributed to 20.66% of the overall variation within the sample. Principal Components 3 and 4 exhibited variability of 9.87% and 8.92%, respectively. The third Principal Component exhibited positive loadings on Depth (+0.509), pH (+0.407), and Cl^- (+0.399), whereas Principal Component 4 demonstrated even higher positive loadings on Fe^+ (+0.482) and $NO2^-$ (+0.60) (Table 3).

Table 3. Extracted Eigenvectors using PCA for the study area.

Parameters	PC1	PC2	PC3	PC4
Depth (mbgl)	-0.16966	0.00367	**0.5094**	-0.38121
pH	-0.10537	-0.31207	**0.4074**	0.30602
EC (ds/m)	**0.40489**	-0.02078	0.20622	0.02223
TDS (mg/l)	**0.39546**	0.08868	-0.05109	0.02334
TH (mg/L)	0.12436	**0.40098**	-0.10624	0.28286
Fe(mg/L)	-0.08075	-0.06921	0.28826	**0.48288**
F(mg/L)	0.29055	**-0.29292**	0.22544	0.01201
Cl(mg/L)	0.33913	0.1707	**0.39909**	-0.00362
HCO_3(mg/L)	**0.31394**	-0.28588	-0.30645	0.07597
NO2(mg/L)	-0.16192	0.11734	0.02843	**0.60043**
Ca+Mg (mg/L)	0.18895	**0.43607**	0.16357	-0.2117
K(mg/L)	0.15193	**0.4783**	-0.05666	0.16818
Na(mg/L)	**0.38516**	-0.12591	0.15806	0.08157
Alkalinity (mg/L)	**0.29405**	-0.28897	-0.27432	0.0248

Source: Calculated by authors, Values in bold are significant.

In terms of spatial distribution, lower PC1 scores concentrated in the central segment, while peripheral segments showed higher scores (Figure 10a). Significant positive correlations exist between TDS, EC, HCO_3, Na and Alkalinity with PCA 1. These elements (EC and TDS) originate from agricultural waste and runoff water carrying significant solids that interact with groundwater through percolation (Folarin et al., 2023). Organic materials in the aquifer undergo oxidation generating carbon dioxide, facilitating mineral dissolution and bicarbonate formation. Weathering introduces calcium, magnesium, and bicarbonate ions into groundwater (Arifullah et al., 2022). PC2 scores gradually increased from northwest to southeast (Figure 10b). Liu et al. (2023) identify factors increasing TH concentrations: weathering of sedimentary rocks, heavy lime use in agriculture, and calcium-rich materials examination. Sabti et al. (2023) indicate groundwater fluoride (F-) originates from weathering and leaching of fluoride-containing minerals in rocks and sediments. Groundwater calcium release occurs via chemical processes involving calcic-plagioclase feldspars and pyroxenes. Fallatah and Khattab (2023) note agricultural fertilizers like lime also contain calcium. Groundwater magnesium derives from limestone and ferromagnesian minerals including olivine, pyroxene, amphiboles, and dark micas. Potassium (K) forms from sylvite (KCl) mineral decomposition, particularly clay minerals. Vero et al. (2023) identify fertilizer and livestock/waste decomposition as potassium sources infiltrating groundwater. Figure 10c shows the central study region exhibited lower PC3 scores compared to northern and southern regions.

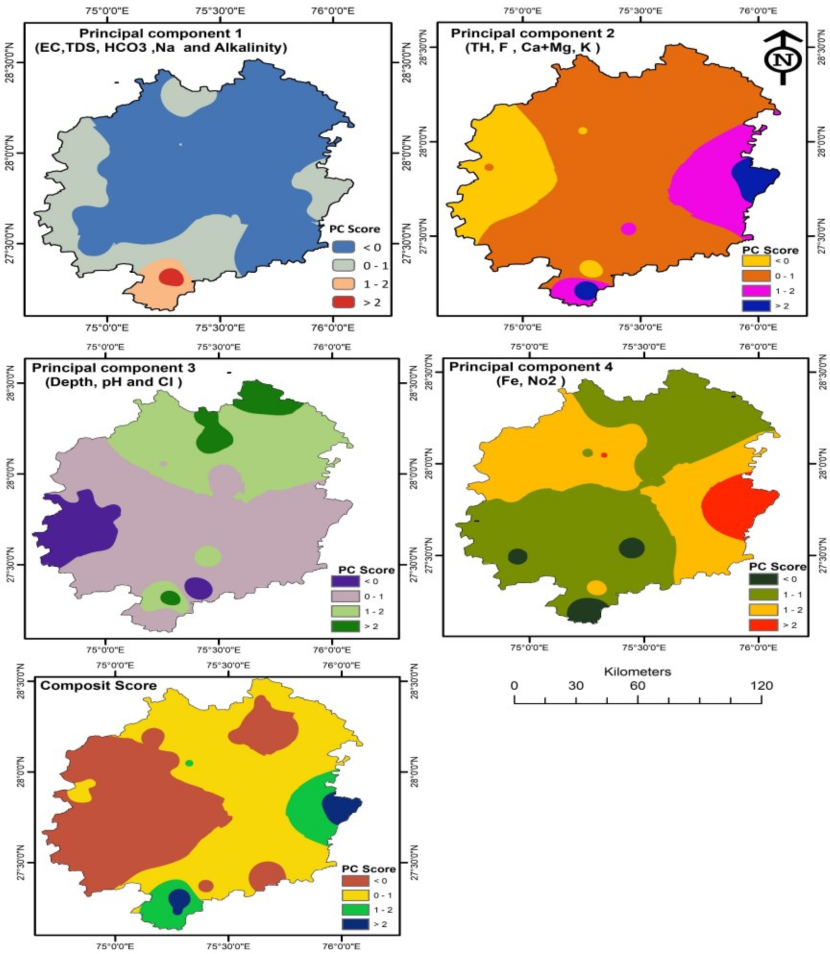

Figure 10. Spatial distribution of Principal Components.

The pH of groundwater significantly influences hydrogeochemical reactions. Irunde et al. (2022) attribute this to sedimentary rock weathering, calcium-containing materials, or excessive agricultural lime application. Groundwater chloride sources include domestic sewage evaporation, industrial waste pollution, or geological formations (Rajmohan et al., 2021). The central region showed notably elevated PC4 scores versus northern and southern regions (Figure 10d). The composite score revealed higher southeastern scores and relatively lower central scores (Figure 10e). Another elevated score area was noted in the northern section. Significant iron (Fe) levels occur in groundwater, especially in tropical areas. Iron typically exists as reduced soluble ferrous iron ($Fe2^{+}$). Atmospheric oxygen contact oxidizes iron to ferric state, precipitating iron minerals. Underlying reducing conditions influence high groundwater Fe concentrations (Zhong et al., 2021). Nitrite plays a crucial fertilizer role. Elevated groundwater nitrogen may result from fertilizers and untreated sewage pollution. Nitrite, positively correlated with effluent discharge and agricultural pesticide overuse, contributes to anthropogenic regional contamination (Brindha and Schneider 2019).

Conclusions

This study evaluated the hydro-geochemical properties of groundwater in Rajasthan's semi-arid and dry region to assess its suitability for domestic and agricultural use. Samples with Na-Cl characteristics indicated significant evaporation processes. The Wilcox diagram showed that many samples ranged from permissible to doubtful in quality. The central area exhibited better water quality compared to neighboring regions. Principal Component Analysis identified four key components explaining most variability in the dataset. The study also suggested a link between groundwater properties, the aquifer medium, and human activities like agriculture. These insights will aid authorities in developing strategies to ensure groundwater safety and accessibility. The research highlights the importance of regular groundwater quality assessments and management. Although focused on a specific area, the methodology and findings can be expanded spatially and by including additional indicators to account for seasonal variations, providing a broader understanding of groundwater conditions in similar regions.

Acknowledgement

The first author acknowledges the University Grants Commission (UGC), Government of India, for providing financial support through the UGC-NET-JRF doctoral fellowship. The authors would like to express their gratitude to Mody University of Science and Technology, Lakshmangarh, Sikar, Rajasthan, India, for the valuable institutional support provided during the course of this research work.

References

Adimalla N, Li P (2019) Occurrence, health risks, and geochemical mechanisms of fluoride and nitrate in groundwater of the rock-dominant semi-arid region, Telangana State, India. *Hum. ecol. risk assess*. 25(1–2): 81–103.

Al Sabti B, Samayamanthula DR, Dashti FM, Sabarathinam C (2023) Fluoride in Groundwater. In Hydrogeochemistry of Aquatic Ecosystems 1–31.

Arifullah, Changsheng H, Akram W, Rashid A, Ullah Z, Shah M, Alrefaei AF, Kamel M, Aleya L, Abdel-Daim MM (2022) Quality Assessment of Groundwater Based on Geochemical Modelling and Water Quality Index (WQI). Water 14(23): 3888.

Brindha K, Schneider M (2019) Impact of Urbanization on Groundwater Quality. In

GIS and Geostatistical Techniques for Groundwater Science 179–196.

Bureau of Indian Standards (BIS) (1991) Indian standard specification for drinking water, IS 10500.

Central Ground Water Board (2017) Aquifer mapping and groundwater management.

Davis JC, Sampson RJ (1986) Statistics and data analysis in geology. Vol. 646.

District Census Handbook Jhunjhunu. (2014) Census of India 2011 - Rajasthan - Series 09 - Part XII B, Directorate of Census Operations, Rajasthan.

District census handbook Sikar (2014) Census of India 2011 - Rajasthan - Series 09 - Part XII B, District Census Handbook, Sikar.

Dong S, Liu B, Chen Y, Ma M, Liu X, Wang C (2022) Hydro-geochemical control of high arsenic and fluoride groundwater in arid and semi-arid areas: A case study of Tumochuan Plain, China. Chemosphere, 301: 134657.

Du W, Wang G (2014) Fully probabilistic seismic displacement analysis of spatially distributed slopes using spatially correlated vector intensity measures. Earthq. Eng. Struct. Dyn. 43(5): 661–679.

Elemile OO, Ibitogbe EM, Folorunso OP, Ejiboye PO, Adewumi JR (2021) Principal component analysis of groundwater sources pollution in Omu-Aran Community, Nigeria. Environ. Earth Sci., 80(20),: 690.

Fallatah O, Khattab MR (2023) Study of hydrogeochemical factors affecting groundwater quality used for land reclamation: application of multivariate statistical analysis. Stoch. Environ. Res. Risk Assess. 37(12): 4719–4735.

Folarin GM, Badmus BS, Akinyemi OD, Idowu OA, Oke AO, Badmus GO (2023) Groundwater quality assessment using physico-chemical parameters and pollution sources apportionment in selected farm settlements of Southwestern Nigeria. *Int. J. Water* Res. Environ. 7(1): 85–103.

Ghosh & Kanchan (2014) Geoenvironmental appraisal of groundwater quality in Bengal alluvial tract, India: a geochemical and statistical approach. Environ. Earth Sci.72(7):2475–2488.

Gugulothu S, Subba Rao N, Das R, Duvva LK, Dhakate R (2022) Judging the sources of inferior groundwater quality and health risk problems through intake of groundwater nitrate and fluoride from a rural part of Telangana, India. Environ. Sci. Pollut. Res. 29(32): 49070–49091.

Helena B (2000). Temporal evolution of groundwater composition in an alluvial aquifer (Pisuerga River, Spain) by principal component analysis. Water Research 34(3): 807–816.

Irunde R, Ijumulana J, Ligate F, Maity JP, Ahmad A, Mtamba J, Mtalo F, Bhattacharya P (2022) Arsenic in Africa: potential sources, spatial variability, and the state of the art for arsenic removal using locally available materials. *Groundw. Sustain. Dev*. 18: 100746.

Jolliffi I (2002). Principle Component Analysis, 2nd edition, Springer, p 518

Kar A. (2014) Agricultural land use in arid Western Rajasthan: Resource exploitation and emerging issues. Agropedology 24(2): 179–196.

Kheirandish M, Rahimi H, Kamaliardakani M, Salim R (2020) Obtaining the effect of sewage network on groundwater quality using MT3DMS code: Case study on Bojnourd plain. *Groundw. Sustain. Dev* 11: 100439.

Kumar A, Singh S, Pramanik M, Chaudhary S, Maurya A K & Kumar M (2022). Watershed prioritization for soil erosion mapping in the Lesser Himalayan Indian basin using PCA and WSA methods in conjunction with morphometric parameters and GIS-based approach. Environment, development and sustainability, 1-39.

Li C, Gao X, Zhang, X, Wang Y, Howard K (2022) Groundwater fluoride and arsenic mobilization in a typical deep aquifer system within a semi-arid basin. J. Hydrol 609: 127767.

Li Q, Lu L, Zhao Q, Hu S (2023) Impact of Inorganic Solutes' Release in Groundwater during Oil Shale In Situ Exploitation. Water 15(1).

Liu Q, Li D, Tang X, Du W (2023) Predictive Models for Seismic Source Parameters Based on Machine Learning and General Orthogonal Regression Approaches. *B seismol soc am113*(6): 2363–2376.

Liu W, Wu Y, Zhong Y, Zhao H (2023) Concentrations, distribution and influencing factors of selenium (Se) in soil of arid and semi-arid climate: A case from Zhangye-Yongchang region, north-western China. *J geochem explor* 250: 107239.

Marghade D, Malpe DB, Subba Rao N (2015) Identification of controlling processes of groundwater quality in a developing urban area using principal component analysis. Environmental Earth Sciences, 74(7): 5919–5933.

Nihalani SA, Behede SN, Meeruty AR (2022) Groundwater quality assessment in proximity to solid waste dumpsite at Uruli Devachi in Pune, Maharashtra. *Water sci technol*, 85(11): 3331–3342.

Nsiri M, Ben Brahim F, Khlifi M, Bouri S (2021) Assessment of the effects of anthropogenic activities on the El Arich groundwater using hydrogeochemistry, GIS and multivariate statistical techniques: A case study of the semi-arid Kasserine region, Tunisia. *Environ. Qual. Manag.*

Panahi G, Eskafi MH, Rahimi H, Faridhosseini A, Tang X (2021) Physical–chemical evaluation of groundwater quality in semi-arid areas: case study—Sabzevar plain, Iran. Sustain. Water Resour. Manag.7(6): 99.

Patra, S., Sahoo, S., Mishra, P., & Mahapatra, S. C. (2018). Impacts of urbanization on land use/cover changes and its probable implications on local climate and groundwater level. Journal of urban management, 7(2), 70-84.

Qiu D, Zhu G, Bhat MA, Wang L, Liu Y, Sang L, Lin X, Zhang W, Sun N (2023) Water use strategy of nitraria tangutorum shrubs in ecological water delivery area of the lower inland river: Based on stable isotope data. J. Hydrol 624: 129918.

Rajmohan N, Masoud MHZ, Niyazi BAM (2021) Impact of evaporation on groundwater salinity in the arid coastal aquifer, Western Saudi Arabia. Catena 196: 104864.

Ravindra B, Subba Rao N, Dhanamjaya Rao EN (2023) Groundwater quality monitoring for assessment of pollution levels and potability using WPI and WQI methods from a part of Guntur district, Andhra Pradesh, India. *Environ dev sustain* 25(12): 14785–14815.

Saxena H (2021). Geography of Rajasthan. Rawat Publication

Shuai G, Shao J, Cui Y, Zhang Q, Guo Y (2021) Hydrochemical Characteristics and Quality Assessment of Shallow Groundwater in the Xinzhou Basin, Shanxi, North China. Water, 13(14):1993.

Subba Rao N, Chaudhary M (2019) Hydrogeochemical processes regulating the spatial distribution of groundwater contamination, using pollution index of groundwater (PIG) and hierarchical cluster analysis (HCA): A case study. *Groundw. Sustain. Dev* 9: 100238.

Subba Rao N, Dinakar A, Sun L (2022) Estimation of groundwater pollution levels and specific ionic sources in the groundwater, using a comprehensive approach of geochemical ratios, pollution index of groundwater, unmix model and land use/land cover – A case study. J. Contam. Hydrol. 248: 103990.

Subba Rao N, Sunitha B, Das R, Anil Kumar B (2022) Monitoring the causes of pollution using groundwater quality and chemistry before and after the monsoon. Phys. Chem. Earth Parts A/B/C, 128: 103228.

Singh S, Kumar A, Negi MS. Hydro-morphological investigations of Neeru watershed using DEM and geospatial techniques. Int J Geogr Geol Environ 2022;4(2):13-23.

Singhal, A., Gupta, R., Singh, A. N., & Shrinivas, A. (2020). Assessment and monitoring of groundwater quality in semi–arid region. Groundwater for sustainable development, 11, 100381.

Sunita & Ghosh T (2024). Groundwater hydro-geochemical inferences and eXplainable Artificial Intelligence augmented groundwater quality prediction in arid and semi-arid segment of Rajasthan, India. Groundw. Sustain. Dev 26: 101272.

Taiyun W, Viliam S (2021). R package “corrplot”: Visualization of a Correlation Matrix (Version 0.92).

Tizro, A. T., & Voudouris, K. S. (2008). Groundwater quality in the semi-arid region of the Chahardouly basin, West Iran. Hydrological Processes: An International Journal, 22(16), 3066-3078.

Tiwari, A. K., Singh, S. K., Singh, A. K., Giri, S., & Mahato, M. K. (2024). Groundwater geochemical investigation and quality assessment for drinking and irrigation uses in Sohagpur coalfield, Madhya Pradesh, India. Environmental Forensics, 25(5), 287-302.

Vero A, Rao BV, Haokip P, Medo T, Keditsu V (2023) Assessment of groundwater quality using hydrochemistry and geospatial techniques in Kohima town, Nagaland. J. Appl. Geochem. 25(1): 40-52.

Wu X, Feng X, Wang Z, Chen Y, Deng Z (2023) Multi-source precipitation products assessment on drought monitoring across global major river basins. Atmos. Res. 295:106982.

Wu X, Guo S, Qian S, Wang Z, Lai C, Li J, Liu P (2022) Long-range precipitation forecast based on multipole and preceding fluctuations of sea surface temperature. Int. J. Climatol.42(15): 8024–8039.

Xu Z, Li X, Li J, Xue Y, Jiang S, Liu L, Luo Q, Wu K, Zhang N, Feng Y, Shao M, Jia K, Sun Q (2022) Characteristics of Source Rocks and Genetic Origins of Natural Gas in Deep Formations, Gudian Depression, Songliao Basin, NE China. ACS Earth Space Chem. 6(7): 1750–1771.

Yin L, Wang L, Li T, Lu S, Tian J, Yin Z, Li X, Zheng W (2023) U-Net-LSTM: Time Series-Enhanced Lake Boundary Prediction Model. Land, 12(10).

Yin L, Wang L, Li T, Lu S, Yin Z, Liu X, Li X, Zheng W (2023) U-Net-STN: A Novel End-to-End Lake Boundary Prediction Model. Land, 12(8).

Zhong D, Ren S, Dong X, Yang X, Wang L, Chen J, Zhao Z, Zhang Y, Tsang DCW, Crittenden JC (2021) Rice husk-derived biochar can aggravate arsenic mobility in ferrous-rich groundwater during oxygenation. Water Res. 200:117264.

Zhou G, Wang Z, Li Q (2022) Spatial Negative Co-Location Pattern Directional Mining Algorithm with Join-Based Prevalence. Remote Sens.14(9).

Zhou G, Zhang H, Xu C, Zhou X, Liu Z, Zhao D, Lin J, Wu G (2023) A Real-Time

Data Acquisition System for Single-Band Bathymetric LiDAR. *EEE Trans. Geosci. Remote Sens*. 61: 1–21.

Zhou G, Zhou X, Chen J, Jia G, Zhu Q (2022) LiDAR Echo Gaussian Decomposition Algorithm for FPGA Implementation. Sens. 22(12).

Zhu G, Liu Y, Shi P, Jia W, Zhou J, Liu Y, Ma X, Pan H, Zhang Y, Zhang Z, Sun Z, Yong L, Zhao K (2022) Stable water isotope monitoring network of different water bodies in Shiyang River basin, a typical arid river in China. Earth System Science Data, 14(8): 3773–3789.

Gibbs, R. J. (1970). Mechanisms controlling world water chemistry. Science, 170(3962), 1088-1090.